Available online at www.sciencedirect.com

ScienceDirect

Procedia CIRP 67 (2018) 428 – 433

www.elsevier.com/locate/procedia

11th CIRP Conference on Intelligent Computation in Manufacturing Engineering, CIRP ICME '17

FE analysis of low density hemp/epoxy composites produced by a new continuous process

Luca Boccarusso[a,*], Massimo Durante[a], Antonio Langella[a], Fabrizio Memola Capece Minutolo[a]

[a]*Department of Chemical, Materials and Industrial Production Engineering, University of Naples "Federico II", Piazzale Tecchio 80, 80125, Napoli, Italy*

* Corresponding author. Tel.: +390817682370; fax: +390817682362. *E-mail address:* luca.boccarusso@unina.it

Abstract

This paper aims to present a new grid composite structure obtained by stacking hemp fabric layers impregnated by resin using a new continuous process. Both the process feasibility and the mechanical properties of the obtained specimens were investigated in terms of tensile and flexural response. In addition, the effect of the superimposition error of the layers, that can affect the density and the mechanical properties of the produced bio-composites, was studied both experimentally and numerically by finite element models (FEM). The results showed that the process is able to produce low density composites possessing interesting specific mechanical properties with a good level of repeatability.

Peer-review under responsibility of the scientific committee of the 11th CIRP Conference on Intelligent Computation in Manufacturing Engineering

Keywords: Biocomposites; Hemp; Manufacturing; Light-weight structures.

1. Introduction

In the last years, considering the increasing environmental awareness and the introduction of new rules and regulations to reduce the environmental impact and reach sustainability, the new products must minimize the environmental impact, so the interest and the subsequent use of eco-friendly materials is grooving more and more in different application fields. This aspect is particularly relevant in the composite manufacturing field, where both synthetic fibers and petroleum polymers are still widely used. In this contest, the use of natural fibers as reinforcement is reaching an increasing attention, indeed a lot of researches have aimed on the study of a range of recyclable materials based on natural fibers such as flax, ramie, sisal, hemp and many more in order to study their possible use as interesting substitute over the conventional ones.

Among various kinds of natural fibres, the hemp one is one of the most promising because of its interesting properties such as the low density, low cost and high specific mechanical properties. In addition, the hemp plant is characterized by the ability of extracting heavy metals from the soil makes and the environmental conditions required from its cultivation allow the easy growth of this plant around the world. Regarding the matrix used for the natural fibre composites manufacturing, its selection is limited by the temperature at which natural fibres degrade. Both thermoset and thermoplastic polymers are coupled with natural fibres and each one highlights its peculiarity characteristics: thermoplastics are capable of being repeatedly softened by the application of heat and hardened by cooling and have the potential to be the most easily recycled, on the other hand a better emphasis of the fibres mechanical properties are generally achieved by using thermosets as matrix.

In fact, thermoset polymers are particularly attractive as matrix materials for natural fibre reinforced composite production as they generally have reactive functional groups that make them compatible with hydrophilic fibre surfaces [1-3]. Among these, the epoxy is one of the most interesting polymer resins that used as matrix for the natural fibre composites shows very high mechanical properties of the final product [3-4].

Several applications as interior and insulation components of hemp/epoxy composites was largely found in literature in particular in the automotive and building sectors [5-8], whilst

Peer-review under responsibility of the scientific committee of the 11th CIRP Conference on Intelligent Computation in Manufacturing Engineering
doi:10.1016/j.procir.2017.12.237

there are few applications as structural components [9] and few works aimed on the study of manufacturing processes (easily implemented in the industry) to produce hemp composites characterized by low density and high specific mechanical properties.
Based on this overview, this work is focused on the manufacturing of lightweight hemp/epoxy composites through a new process easily implemented in industrial production by using hemp fabrics characterized by a large mesh size. To assess their mechanical performances, tensile and bending tests were performed and coupled with FE simulations.

2. Materials and methods

2.1. Materials

The composites under investigation were produced by using an epoxy resin SX10 EVO (provided by Mates [10]) as matrix and a woven hemp fabric having an areal density (GMS) of 380 g/m^2 (supplied by Fidia [11]), as reinforcement.

Considering that the aim was the manufacturing of lightweight hemp composites for their future application as independent semi-structural components or as core for sandwich structures, the mesh of the fabric was enlarged in order to have its lightening and to simplify the resin removal during the manufacturing process. For this purpose, one alternative tow in weft and wrap direction is manually removed from the hemp fabric; therefore, a woven hemp fabric having a GMS equal to around 190 g/m^2 was obtained. Fig.1 shows the woven hemp fabric before and after the mesh enlargement.

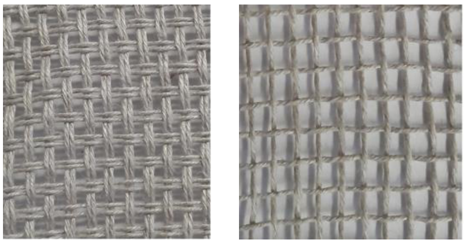

a) b)

Fig. 1. Woven hemp fabric (a) before and (b) after the enlargement of the mesh.

2.2. Experimental procedure

Before the impregnation step, the fabrics were soaked in 2% of NaOH solution at room temperature for 30 min. After treatment, fibres were copiously washed with water to remove any traces of alkali on the fibres surface and subsequently neutralized with 1% acetic acid solution. Then, the treated fibres were dried in an oven at 60°C for 12 h [4].

The composites laminates were manufactured according to the process explained in the patent Nr. 102017000052513.

The process is divided in five main steps:

- Impregnation;
- resin absorption;
- resin content reduction;
- cutting;
- stacking and polymerization.

This technique was used to obtain impregnated grid hemp fabric layers. Each hemp layers, for a total number of four, were impregnated with the epoxy resin according to the described process, keeping the hemp weight fraction equal to around 36 wt.% for each layer. Table 1 summarizes the sample typologies under investigation.

Table 1 Laminates typologies details.

Sample type	Fabric type	Number of layers
A	Standard	4
B	Enlarged	4

2.3. Mechanical characterization

Tensile tests were carried out according to ASTM 3039 standard, then specimens with a width of 25 mm, an overall length equal to 250 mm and a tab length of 50 mm were tested under a crosshead displacement of 1 mm/min.

The flexural properties were investigated in three-point bending test conditions. These tests were performed according to ASTM D790-10, then the span length to thickness ratio was set equal to 16 and the specimen width was always 35 mm. All tests were performed at constant crosshead displacement of 0.5 mm/min.

In addition, in order to obtain the mechanical properties of the single impregnated tow, required as input data for the finite element (FE) models, tensile tests on impregnated tows were also carried out (Fig 2a). Finally, to guarantee the reliability of the FE models, tensile tests on specimens constituted by a single impregnated layer were also performed (Fig. 2b).

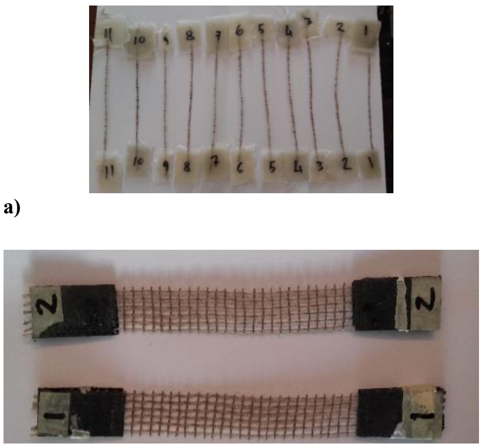

a)

b)

Fig. 2. Impregnated tows specimens (a) and single impregnated layer specimens (b) for tensile tests.

2.4. FE models

In order to justify the flexural behaviour of B type composites, FE simulations were carried out by using LS-Dyna as software. In this contest, the simulations were performed in two different conditions that mainly differs in the specimen configuration: in the first one there is a perfect alignment among the different fabric layers (Fig. 3), whilst in the second one it was taken into account a possible misalignment error (Fig. 4).

To make as truthfully as possible the geometry of the used fabric, the surface of an impregnated fabric layer was acquired by using a confocal microscope (LEICA DCM 3D). According to the technique described in [12], a CAD model of the single cell of the fabric can be obtained and then meshed, as shown in Fig. 5.

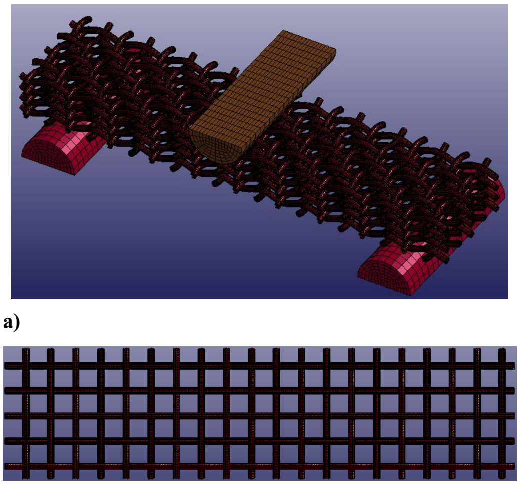

Fig. 3. FEM of the three-point bending test in the perfect alignment condition (a) and top view of the specimen model (b).

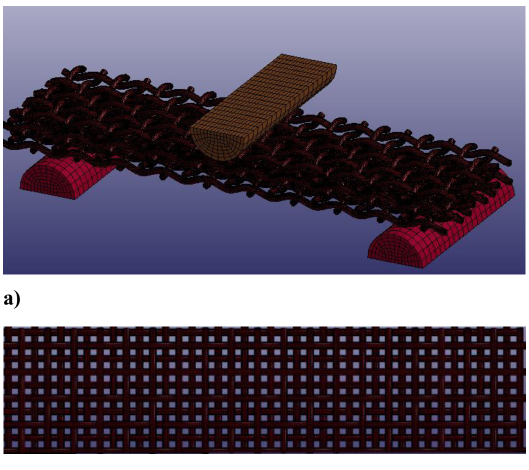

Fig. 4. FEM of the three-point bending test considering a possible misalignment error (a) and top view of the specimen model (b).

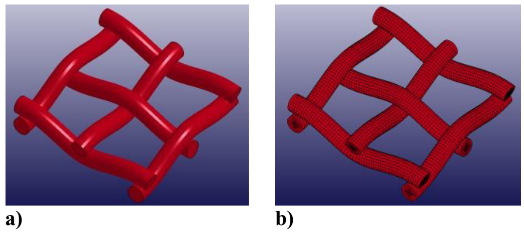

Fig. 5. CAD model of the unit cell (a) and its mesh (b).

The FE simulations were carried out using the implicit solver of LS-Dyna and MAT 03 (plastic_kinematics) as material card for the single tow, considering failure elongation conditions. In order to validate the mesh and the material data inserted in the FE models, tensile test on a single impregnated layer was also simulated and the results were compared to the experimental one. Considering the load symmetry conditions, only half specimen was modeled.

3. Results and discussions

Table 2 summarized the typologies of the obtained samples and their main characteristics, and Fig. 6 shows the top surface of the two sample types. The fiber volume fraction, V_f, was evaluated according to equation (1) where ρ_f is the fibers density equal to 1.5 g/cm^3 and W_f and ρ_c are the fiber weight fraction and the composite density respectively.

$$V_f = \frac{\rho_c}{\rho_f} W_f \tag{1}$$

Table 2 Produced laminates types and their properties.

Sample type	Mean thickness [mm]	W_f [%]	ρ_c [g/cm^3]	V_f [%]
A	5.3	38	0.74	19
B	4.3	38	0.47	12

Firstly, it is possible to note that the despite the same number of layers was used for each sample type, the mean thickness is different. This is due to the occurrence of misalignment errors, during the stack step of the manufacturing process, among the different layers of the laminate.

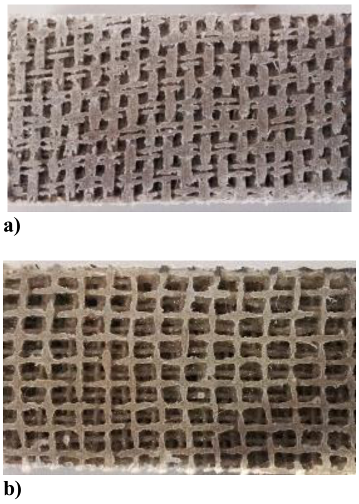

Fig. 6. Typical top surface of the specimens of A type (a) and B type (b).

This is clear looking at Fig. 7 where both an ideal superimposition case and the one affects by a superimposition error are showed.

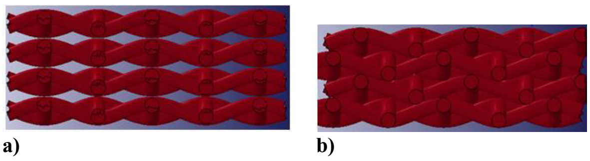

Fig. 7. Cross section of a sample with an ideal superimposition stack step (a) and the one where a possible misalignment error is considered (b).

Therefore, due to the no optimum control in the fabric superimposition, even though the fibre weight content is the same for each sample typology, the difference in the thickness vales is directly connected with the difference in the density and in the fibre volume fraction values. Ideally, considering for the B type a good alignment able to obtain the same thickness of the A type sample and also considering that the B type samples contained half number of tows then the A type, the ideal values of the density and of the fabric volume fraction should be half than the ones of the A type.

Figs. 8 and 9 shows the tensile and bending stress-strain curves for the specimens under investigation. The composites with density of around 0.74 g/cm^3 are characterized by a tensile strength of 40 MPa and a tensile modulus of 3000 MPa, whilst the composites with a density of around 0.47 g/cm^3 showed a tensile strength of 24 MPa and a tensile modulus of 1650 MPa; the tensile properties of the B type are approximately half of the ones of the A type.

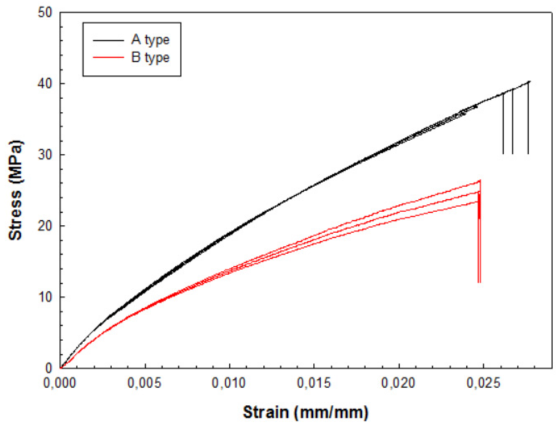

Fig. 8. Tensile stress-strain curves.

Looking at Fig. 9, it is possible to note that all curves show the same behavior up to the failure, but when the maximum stress value was reached and then the specimens started to fail, the behavior changes. This is observed by comparing the stress-strain curves and the type of failure of the specimens show in Fig. 10. The curves of the A type show a significant drop in the stress and then a brittle failure of the specimens was observed, whilst the curves of the B type show a slighter decrease in the stress coupled with a sliding failure. This is due to the higher presence of resin on the bottom surface of the A type specimens. The composites with a density of 0.77 g/cm^3 showed a bending strength of 40 MPa and a bending modulus of 3100 MPa, instead of the samples with a density of around 0.47 g/cm^3 that was characterized by a bending strength of 22 MPa and a bending modulus of 1200 MPa.

It is also possible to observe that the flexural mechanical response variability is in any case quite limited. However, a slightly greater value was reached for the B type specimens due to above said misalignment problems that mainly occurs for this specimen typology. This is also corroborated from the results of the FE simulations of the three-point bending tests where the eventual misalignment error was considered.

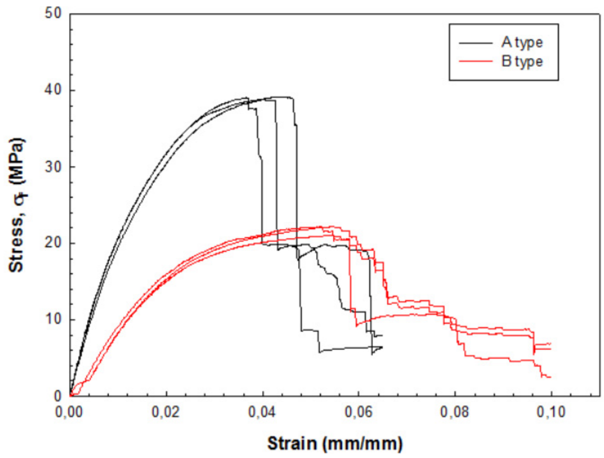

Fig. 9. Flexural stress-strain curves.

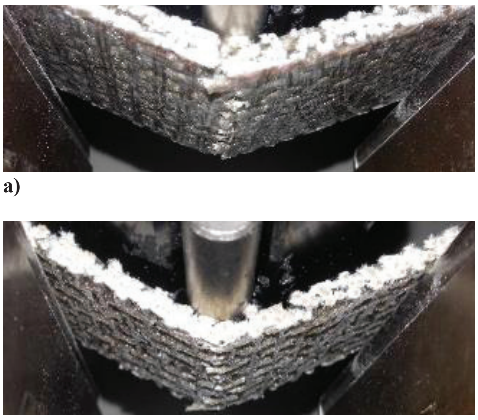

Fig. 10. Samples of the A (a) and B (b) type at the end of the bending test.

Concerning the results of the FE simulations, a first validation of the model was done by comparing the experimental and the numerical results of the tensile tests carried out on the single impregnated layer. In Fig. 11 both the experimental and the numerical load-displacement curves were plotted and from their comparison it is possible to evince the good reliability of the FE model.

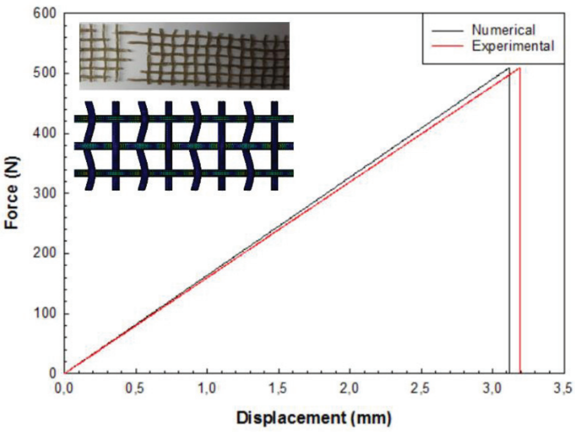

Fig. 11. Experimental and numerical tensile force-displacement curves.

After this first validation, it is possible to illustrate the results of the three-point bending test simulations. Fig. 12 shows a comparison in terms of flexural load-displacement curves among the numerical and the experimental tests.

It is possible to note that the misalignment error affects the flexural mechanical response in a predictable way, indeed all the experimental curves were comprised between the numerical ones; highlighting that the top numerical curve represents an ideal configuration. This means that although the occurring of a lack of control in the superimposition of each layer, at least in the case where four fabric layers were used, this error does not affect so much the flexural response.

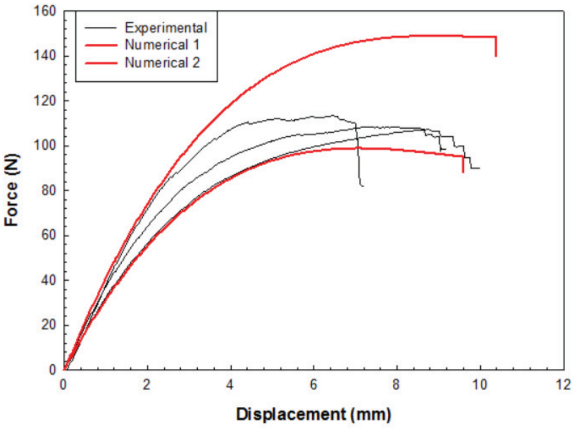

Fig. 12. Experimental and numerical flexural force-displacement curves.

4. Conclusions

The proposed method (continuous impregnation process) was used to produce hemp/epoxy composites with different density values, using two type of woven hemp fabric characterized by two different meshes. By using this method, composites with a density range of 0.47-0.74 g/cm^3 (it depends on the type of fabric used) and a fixed hemp fiber weight ratio equal to 38% were produced with a high level of repeatability.

This one represents an interesting advantage of this technique, that can be easily implemented in the industrial production. The good process repeatability was directed reflected on the mechanical properties repeatability, showing also a good relation between the experimental and the numerical response.

A possible process criticality is the misalignment in the layer superimposition during the stack step that mainly affects the sample typology characterized by the largest mesh size. This could involve effects on the thickness values variability and therefore on the specimen density.

However, from the results of both the FE simulations and the experimental tests, it was observed that in the case under study and then by using four fabric layers, the occurring of this possible error does not affect so much the mechanical properties.

Considering the above reported values, the proposed lightweight hemp composite products could be used for future applications both as core for sandwiches and as independent semi-structural components. In future woks, it could be interesting to increase the thickness of the samples, by augmenting the number of layers, in order to study if/how the thickness affects the mechanical and physical properties of the proposed grid structure.

References

[1] Summerscales J, Dissanayake N, Virk A and Hall W. A review of bast fibres and their composites. Part 1 – fibres as reinforcements. Comp Part A 2010;41:1329-35.

[2] Pickering K, Aruan Efendy M and Le T. A review of recent developments in natural fibre composites and their mechanical performance. Comp Part A 2016;83:98-112.
[3] Sepe R, Bollino F, Boccarusso L, Caputo F. Influence of chemical treatments on mechanical properties of hemp fiber reinforced composites. Comp Part B 2018;133:210-7
[4] Boccarusso L, Carrino L, Durante M, Formisano A, Langella A, Memola Capece Minutolo F. Hemp fabric/epoxy composites manufactured by infusion process: Improvement of fire properties promoted by ammonium polyphosphate. Comp Part B 2016; 89:117-26.
[5] Holbery J and Houston D. Natural-fiber-reinforced polymer composites in automotive applications. JOM 2006;58:80-86.
[6] Rohit K and Dixit S. A Review - Future Aspect of Natural Fiber Reinforced. Polymers from Renewable Resources 2016;7:43-59.
[7] Mohanty AK, Misra M and Drzal LT. Sustainable bio-composites from renewable resources: Opportunities and challenges in the green materials world. Journal of Polymers and the Environment 2002;10:19-26.
[8] Menna C, Aprone D, Durante M, Zinno A, Balsamo A, Prota A. Structural behavior of masonry panels strengthened with an innovative hemp fibre composite grid, Constr Build Mater 2015;100:111-21
[9] Boccarusso L, Carrino L, Durante M, Formisano A, Langella A, and Memola Capece Minutolo F, Innovative core material produced by infusion process using hemp fibres, AIP Conference Proceedings 2016;1769: 170025.
[10] Characteristics of the used epoxy resin available at: http://www.mates.it/indexingl.html;2014.
[11] Characteristics of the used hemp fabric available at: http://www.fidiaglobalservice.com/eng/materiali.htm;2014.
[12] Boccarusso L, Arleo G, Astarita A, Bernardo F, De Fazio P, Durante M, Memola Capece Minutolo F, Sepe R, Squillace A. A new approach to study the influence of the weld bead morphology on the fatigue behaviour of Ti–6Al–4V laser beam-welded butt joint. Int J Adv Manuf Technol 2017; 88:75–88.